

## **Molecular interactions of ionic liquids with SiO<sub>2</sub> surfaces determined from colloid probe atomic force microscopy**

Yudi Wei<sup>a,‡</sup>, Zhongyang Dai<sup>b,‡</sup>, Yihui Dong<sup>c,‡</sup>, Andrei Filippov<sup>d,e</sup>, Xiaoyan Ji<sup>f</sup>, Aatto Laaksonen<sup>f,g,h,i</sup>, Faiz Ullah Shah<sup>d</sup>, Rong An<sup>a,\*</sup> and Harald Fuchs<sup>a,j</sup>

<sup>a</sup> Herbert Gleiter Institute of Nanoscience, Department of Materials Science and Engineering, Nanjing University of Science and Technology, Nanjing 210094, P.R. China

<sup>b</sup> High Performance Computing Department, National Supercomputing Center in Shenzhen, Shenzhen 518055, Guangdong, P. R. China

<sup>c</sup> Department of Molecular Chemistry and Materials Science, Weizmann Institute of Science, Rehovot 76100, Israel.

<sup>d</sup> Chemistry of Interfaces, Luleå University of Technology, 97187 Luleå, Sweden

<sup>e</sup> Medical and Biological Physics, Kazan State Medical University, 420012 Kazan, Russia

<sup>f</sup> Energy Engineering, Division of Energy Science, Luleå University of Technology, 97187 Luleå, Sweden

<sup>g</sup> Division of Physical Chemistry, Department of Materials and Environmental chemistry, Arrhenius Laboratory, Stockholm University, Stockholm 10691, Sweden

<sup>h</sup> Center of Advanced Research in Bionanoconjugates and Biopolymers, “Petru Poni” Institute of Macromolecular Chemistry, Iasi 700469, Romania

<sup>i</sup> State Key Laboratory of Materials Oriented and Chemical Engineering, Nanjing Tech University, Nanjing 211816, P. R. China.

<sup>j</sup> Center for Nanotechnology (CeNTech), Institute of Physics, Westfälische Wilhelms-Universität Münster, 48149 Münster, Germany

<sup>‡</sup> Yudi Wei, Zhongyang Dai, and Yihui Dong contributed equally to this work.

\*Corresponding Author: Rong An, Email: [ran@njust.edu.cn](mailto:ran@njust.edu.cn)

## 1. Predicting diffusion coefficients with CG-MD simulations.

Lennard-Jones 12-6 (equation 1) potential was used to describe the interaction between the single-bead IL ion pairs,

$$E = 4\varepsilon\left[\left(\frac{\sigma}{r}\right)^{12} - \left(\frac{\sigma}{r}\right)^6\right] \quad (1)$$

where  $r$  refers to the distance between two IL ion pairs,  $\varepsilon$  and  $\sigma$  represent, respectively, the parameters of size and energy well depth.

Similarly, the interaction between the IL and SiO<sub>2</sub> was also described using the Lennard-Jones wall potential, as shown in equation (2), where  $d$  represents the distance of a specific CG ion pair bead to the SiO<sub>2</sub> wall.

$$E = 4\varepsilon\left[\left(\frac{\sigma}{d}\right)^{12} - \left(\frac{\sigma}{d}\right)^6\right] \quad (2)$$

The energy parameter, *i.e.*, the interaction strength between the IL and SiO<sub>2</sub>,  $\varepsilon_{IL-SiO_2}$ , was taken directly from the CP-AFM-derived force, converted to potential well depth of the IL with SiO<sub>2</sub> (Table 4). The size parameters,  $\sigma_{IL}$ , reflecting the estimated effective diameters of the single-bead cation-anion pairs, are 0.68 nm<sup>1</sup> and 0.70 nm<sup>2</sup> for BB and BP, respectively.

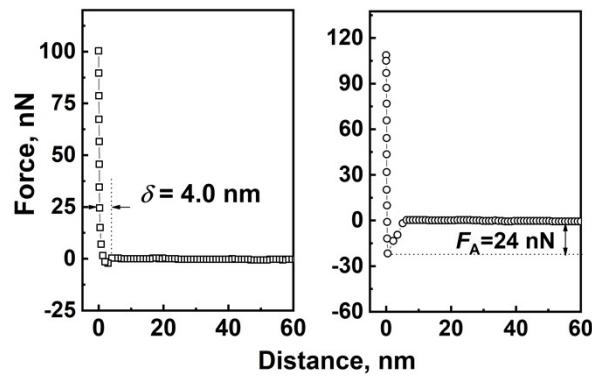


**Figure S1.** Representative approaching (left) and retracting (right) force-distance curves for the SiO<sub>2</sub> colloid probe with SiO<sub>2</sub> microsphere.

**Table S1.** Parameters for calculating molecular interactions of SiO<sub>2</sub> with SiO<sub>2</sub>

$F_{A, SiO_2}$ , nN <sup>a</sup>	$25.3 \pm 2.20$
$\delta_{SiO_2}$ , nm <sup>b</sup>	$4.53 \pm 0.51$
$A_{SiO_2}$ , m <sup>2</sup> <sup>c</sup>	$1.42 \times 10^{-13}$
$F_{A, SiO_2}^*$ , nN/m <sup>2</sup> <sup>d</sup>	$1.78 \times 10^{14}$
$F_{A, SiO_2-g}$ , nN/g <sup>e</sup>	$1.80 \times 10^{16}$
$F_{A, SiO_2-m}$ , nN/mol <sup>f</sup>	$1.08 \times 10^{18}$
$F_{0, SiO_2}$ , nN/Num <sup>g</sup>	$1.79 \times 10^{-6}$
$\sigma_{SiO_2}$ , nm <sup>h</sup>	0.27
$\epsilon_{SiO_2}$ , kcal/mol <sup>i</sup>	0.0695

<sup>a</sup>  $F_{A, SiO_2}$ , nN, the net adhesion force measured by AFM between SiO<sub>2</sub> colloid probe and SiO<sub>2</sub> microspheres (the radius  $R$  of SiO<sub>2</sub> is 10 μm).

<sup>b</sup>  $\delta_{SiO_2}$ , nm, the indentation depth of SiO<sub>2</sub> colloidal probe interacting with the SiO<sub>2</sub> microsphere.

<sup>c</sup>  $A_{SiO_2}$  ( $A_{SiO_2} = \pi \times \delta(\times 10^{-9}) \times R(\times 10^{-6})$ ), m<sup>2</sup>, the effective contact area of SiO<sub>2</sub> colloidal probe interacting with the SiO<sub>2</sub> microsphere, based on Hertz model.

<sup>d</sup>  $F_{A, SiO_2}^*$  ( $F_{A, SiO_2}^* = \frac{F_{A, SiO_2}}{A_{SiO_2}}$ ), nN/m<sup>2</sup>, the interaction of SiO<sub>2</sub> microsphere interacting with the SiO<sub>2</sub> colloid probe per unit area.

<sup>e</sup>  $F_{A, SiO_2-g}$  ( $F_{A, SiO_2-g} = F_{A, SiO_2}^* \times S_{SiO_2}$ ), nN/g, the interaction of SiO<sub>2</sub> microsphere interacting with the SiO<sub>2</sub> colloid probe per gram. The BET surface area of SiO<sub>2</sub> microspheres  $S_{SiO_2} = 100.9 \pm 2.67$  m<sup>2</sup>/g.

<sup>f</sup>  $F_{A, SiO_2-m}$  ( $F_{A, SiO_2-m} = F_{A, SiO_2-g} \times M_{SiO_2}$ ), nN/mol, the interaction of SiO<sub>2</sub> microsphere interacting with the SiO<sub>2</sub> colloid probe per mole. The molecular weight of SiO<sub>2</sub>,  $M_{SiO_2} = 60$  g/mol.

<sup>g</sup>  $F_{0, SiO_2}$  ( $F_{0, SiO_2} = \frac{F_{A, SiO_2-m}}{N_A}$ ), nN/Num, molecular interactions of SiO<sub>2</sub> with SiO<sub>2</sub>.

<sup>h</sup>  $\sigma_{SiO_2}$ , nm, the molecular parameter of SiO<sub>2</sub>.

<sup>i</sup>  $\epsilon_{SiO_2}$  ( $\epsilon_{SiO_2} = \frac{F_{0, SiO_2}(\times 10^{-9}) \times \sigma_{SiO_2}(\times 10^{-9}) \times N_A}{4.184(\times 10^3)}$ ), kcal/mol, potential well depth.

MD simulation provides the trajectories of the ILs, from which the diffusion coefficient  $D$  can be extracted based on the Einstein relationship:<sup>3,4</sup>

$$D = \frac{1}{6} \lim_{t \rightarrow \infty} \frac{d}{dt} \langle |r(t) - r(0)|^2 \rangle \quad (3)$$

where  $\langle |r(t)-r(0)|^2 \rangle$  is the ion's mean square displacement inside the pores, and the diffusion coefficient is obtained from the mean slope of the mean squared displacement as time goes to infinity. We assume a diffusion in three dimension inside the pores, whereby we use factor 6 in the Einstein relationship in Equation (3). Self-diffusion is directly proportional to temperature and inversely proportional to the mass of the diffusing particle. All deviations from this behaviour come from external sources and environment.

## 2. Measuring diffusion coefficients with NMR.

To find out the reliability of the AFM-quantified molecular interactions of ILs with SiO<sub>2</sub>, the temperature-dependent diffusion coefficient changes of ILs confined in nanoporous glasses were measured experimentally by NMR diffusometry. As both cations and anions and their diffusion can be followed separately in NMR it is also a good control how rude is the approximation in the CG potential model not to treat them separately and to assume them to diffuse as connected ion pairs. To compare with simulations we use the average of cation and anion diffusion. The diffusion of cations was studied by <sup>1</sup>H NMR in all ILs, and that of anions was studied by <sup>11</sup>B NMR in BB and by <sup>31</sup>P NMR in BP. Diffusion in BB was measured only to 363 K in the pores of Varapor and 333 K in Vycor, due to the destruction of BB at higher temperatures. The averaged diffusion coefficient of ILs ( $D$ ) can be obtained by equation (4),

$$D = 0.5 \times (D_{\text{cation}} + D_{\text{anion}}) \quad (4)$$

where  $D_{\text{cation}}$  and  $D_{\text{anion}}$  are the diffusion coefficients of cations and anions, respectively.

The temperature-dependent diffusion coefficients of ILs for the confined ILs in nano-porous glasses measured by NMR are presented in Figure S2, showing the diffusion is enhanced at a higher temperature. Compared to those for the ILs in bulk,

the confinement of the ILs in pores leads to a decrease of diffusion coefficient for both BB and BP. The magnitude of the decrease is higher in SiO<sub>2</sub> with smaller pore size (4 nm) than that in the one with pore size of 10 nm.

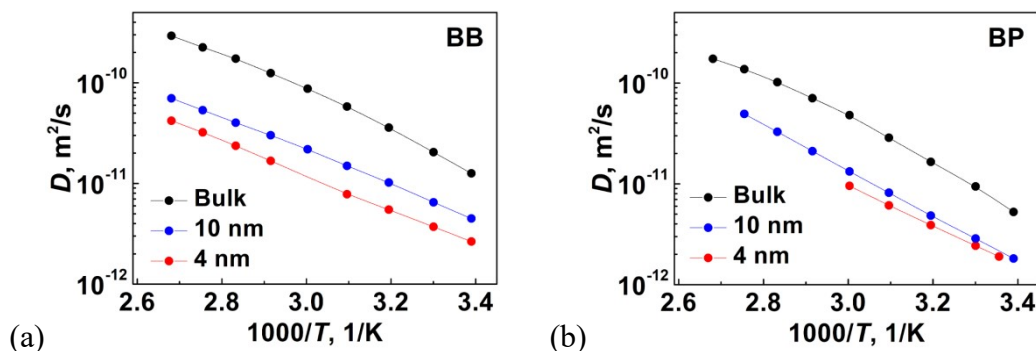


**Figure S2.** Diffusion coefficient of the ILs in the bulk and confined in Vycor with 4 nm cylindrical pores and Varapor with 10 nm cylindrical pores at different temperatures measured by NMR: (a) BB, (b) BP.

### 3. Simulation details.

To develop an approximate force field model to describe the two ILs BB and BP and their interactions in this work, we start from a force field of imidazolium-based ILs, developed by Liu et al.,<sup>5</sup> but we follow the strategy from PC-SAFT type models by creating hard-sphere beads in the coarse-graining.<sup>6</sup> We present a very simplified IL model where each ion-pair is approximated as an independent spherical particle with zero charges using Lennard-Jones 12-6 interaction potentials for the interactions, *i.e.*, between the IL ion pairs, as well as between the IL and SiO<sub>2</sub>. The number of confined ion pairs was calculated using an effective volume, based on the bulk density of ILs<sup>7,8</sup> in the channels, which accurately estimates the density of the confined ILs.

**Table S2.** The simulation box size and IL particle number used in the simulation.

	pore size (nm)	length_x (nm)	length_y (nm)	length_z (nm)	particle number
BB	4	10	10	50	2025
	10	20	20	60	15187
BP	4	10	10	50	1837
	10	20	20	60	13776

The self-diffusion coefficients of BB and BP ILs, confined in the 4 nm and 10 nm SiO<sub>2</sub> cylindrical channels, respectively, were investigated at different temperatures by MD simulations. The size of simulation box and IL particle number used in the simulation is listed in Table S2, and the representative configuration of BP particles confined in the cylindrically porous SiO<sub>2</sub> with 10 nm pore is shown in Figure S3. In prior to each simulation, an equilibration of 30 ns was performed in a canonical (NVT) ensemble to optimize the box. The time step was 1.0 fs and the temperature was kept constant via Nose–Hoover thermostat with a damping time of 100.0 fs. The periodic boundary conditions (PBC) were applied in the direction parallel to the cylinder axis. After that, another 10 ns calculation at each temperature was performed to collect the trajectory coordinates of particles with a storage frequency of 100 steps. These trajectories were analyzed to compute the diffusion coefficients of the ILs under confinement from mean square displacement using the Einstein equation.<sup>3, 4</sup> All simulations were performed using the large-scale atomic/molecular massively parallel simulator (LAMMPS) package.<sup>9</sup>

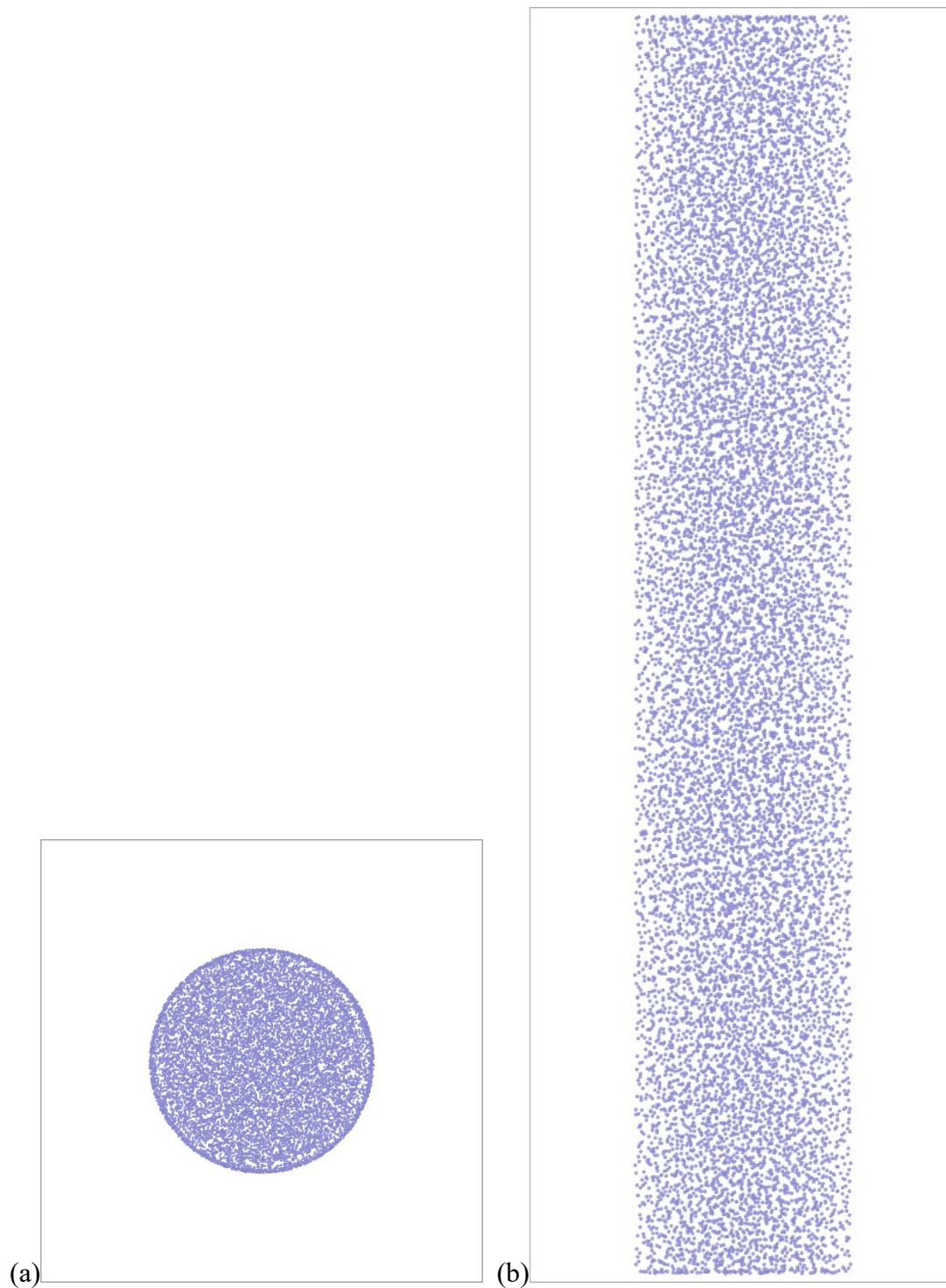


**Figure S3** Representative configuration of BP particles confined in the cylindrically porous SiO<sub>2</sub> with 10 nm pore: (a) top (x-y) view and (b) side (x-z) view.

#### **4. Measurement of diffusion coefficient using NMR diffusometry.**

Pulsed gradient spin echo (PGSE) NMR diffusometry was used to study the diffusion of ILs confined in glass (SiO<sub>2</sub>) pores. Two kinds of glasses with cylindrical pores, i.e.,

Vycor 7930 and Varapor100, were firstly cleaned in a boiling 50% hydrogen peroxide aqueous solution at 393 K for 48 h, and then washed with distilled water, dried under vacuum. These glasses were activated at 723 K for 2 h, and then cooled in a bath with the studied ILs under vacuum, finally under atmospheric pressure for two days at 294 K. After that, the sample was removed from the bath, wiped with filter paper, and placed in a glass sample tube, where the sample was heated to 330 K and maintained for 3 h to homogenize the distribution of the IL inside the pores.

With the as-prepared ILs confined by porous glasses, NMR self-diffusion measurements were performed on  $^1\text{H}$  (400.220 MHz),  $^{11}\text{B}$  (128.403 MHz) and  $^{31}\text{P}$  (161.988 MHz) with a PGSE-NMR probe Diff50 (Bruker). PGSE-NMR measurements were performed on a Bruker Avance III (Bruker BioSpin AG) NMR spectrometer. The bulk ILs or porous glass confined ILs were placed in a standard 5 mm glass sample tube and closed with a plastic stopper to avoid air contact. Before the measurements, the samples were equilibrated at a specific temperature for 15 min. The diffusional decays were recorded using the stimulated echo pulse train. Details of the pulsed field gradient NMR technique used for measuring molecular diffusion can be found elsewhere.<sup>10, 11</sup> Briefly, the primary information for the diffusion study by NMR is contained within the diffusion decay (DD) of the NMR spin-echo or stimulated echo amplitude. For the Ste pulse sequence, the diffusion decay ( $A$ ) in the case of a single-component diffusion can be described by equation (5):<sup>11</sup>

$$A(2\tau, \tau_1, g, \delta) = \frac{I}{2} \exp\left(-\frac{2\tau}{t_2} - \frac{\tau_1}{t_1}\right) \exp\left(-\gamma^2 \delta^2 g^2 D t_d\right) \quad (5)$$

where  $I$  is the factor proportional to the proton content in the system;  $t_1$  and  $t_2$  are spin-lattice and spin-spin relaxation times, respectively;  $\tau$  and  $\tau_1$  are time intervals in the pulse sequence;  $\gamma$  is the gyromagnetic ratio for the measured nuclei;  $g$  and  $\delta$  are the amplitude and duration of the gradient pulse, respectively;  $t_d = (\Delta - \delta/3)$  is the diffusion time;  $\Delta = (\tau + \tau_1)$  is the time interval between two gradient pulses; and  $D$  is the self-diffusion coefficient. Measurements were carried out at  $\delta = 1-3$  ms,  $\Delta = 5-30$  ms, the repetition time is 2 s, the amplitude of the pulse gradient  $g$  was chosen considering the values of the diffusion coefficients,  $g_{\max} = 29.7$  T/m.

## References

- 1 H. Li, R. Sedev and J. Ralston, *Phys. Chem. Chem. Phys.*, 2011, **13**, 3952-3959.
- 2 J. Comtet, Ph.D, Université Paris sciences et lettres, 2018.
- 3 A. Moradzadeh, M. H. Motevaselian, S. Y. Mashayak and N. R. Aluru, *J. Chem. Theory Comput.*, 2018, **14**, 3252-3261.
- 4 Y. He, R. Qiao, J. Vatamanu, O. Borodin, D. Bedrov, J. Huang and B. G. Sumpter, *J. Phys. Chem. Lett.*, 2016, **7**, 36-42.
- 5 Z. P. Liu, S. P. Huang and W. C. Wang, *J. Phys. Chem. B*, 2004, **108**, 12978-12989.
- 6 G. Shen, A. Laaksonen, X. Lu and X. Ji, *J. Phys. Chem. C*, 2018, **122**, 15464-15473.
- 7 Z. Dai, L. Shi, L. Lu, Y. Sun and X. Lu, *Langmuir*, 2018, **34**, 13449-13458.
- 8 R. Singh, J. Monk and F. R. Hung, *J. Phys. Chem. C*, 2010, **114**, 15478-15485.
- 9 S. Plimpton, *J. Comput. Phys.*, 1995, **117**, 1-19.
- 10 A. Filippov, N. Azancheev, F. U. Shah, S. Glavatskih and O. N. Antzutkin, *Microporous Mesoporous Mater.*, 2016, **230**, 128-134.
- 11 P. T. Callaghan, *Principles of Nuclear Magnetic Resonance Microscopy*, Oxford Press, Clarendon, 1991.